TRPA1 activation in a human sensory neuronal model: relevance to cough hypersensitivity?

Rebecca Clarke[1], Kevin Monaghan[1], Imad About[2], Caoimhin S. Griffin[3], Gerard P. Sergeant[3], Ikhlas El Karim[1], J. Graham McGeown[1], S. Louise Cosby[1], Timothy M. Curtis[1], Lorcan P. McGarvey[1,4] and Fionnuala T. Lundy[1,4]

Affiliations: [1]Centre for Experimental Medicine, Wellcome-Wolfson Institute for Experimental Medicine, School of Medicine, Dentistry and Biomedical Sciences, Queen's University, Belfast, UK. [2]Aix Marseille Université, CNRS, ISM UMR 7287, , Marseille, France. [3]Smooth Muscle Research Centre, Dundalk Institute of Technology, Dundalk, Ireland. [4]Joint senior authors.

Correspondence: Lorcan P. McGarvey, Centre for Experimental Medicine, Wellcome-Wolfson Institute for Experimental Medicine, School of Medicine, Dentistry and Biomedical Sciences, 97 Lisburn Road, Belfast BT9 7BL, UK. E-mail: l.mcgarvey@qub.ac.uk

@ERSpublications
Development of a novel human adult stem cell neuronal model to investigate neural hyperresponsiveness in cough http://ow.ly/Ilvb30eokUC

Cite this article as: Clarke R, Monaghan K, About I, *et al*. TRPA1 activation in a human sensory neuronal model: relevance to cough hypersensitivity? *Eur Respir J* 2017; 50: 1700995 [https://doi.org/10.1183/13993003.00995-2017].

ABSTRACT The cough reflex becomes hyperresponsive in acute and chronic respiratory diseases, but understanding the underlying mechanism is hampered by difficulty accessing human tissue containing both nerve endings and neuronal cell bodies. We refined an adult stem cell sensory neuronal model to overcome the limited availability of human neurones and applied the model to study transient receptor potential ankyrin 1 (TRPA1) channel expression and activation.

Human dental pulp stem cells (hDPSCs) were differentiated towards a neuronal phenotype, termed peripheral neuronal equivalents (PNEs). Using molecular and immunohistochemical techniques, together with Ca^{2+} microfluorimetry and whole cell patch clamping, we investigated roles for nerve growth factor (NGF) and the viral mimic poly I:C in TRPA1 activation.

PNEs exhibited morphological, molecular and functional characteristics of sensory neurons and expressed functional TRPA1 channels. PNE treatment with NGF for 20 min generated significantly larger inward and outward currents compared to untreated PNEs in response to the TRPA1 agonist cinnamaldehyde ($p<0.05$). PNE treatment with poly I:C caused similar transient heightened responses to TRPA1 activation compared to untreated cells.

Using the PNE neuronal model we observed both NGF and poly I:C mediated sensory neuronal hyperresponsiveness, representing potential neuro-inflammatory mechanisms associated with heightened nociceptive responses recognised in cough hypersensitivity syndrome.

This article has supplementary material available from erj.ersjournals.com

Received: May 15 2017 | Accepted after revision: July 16 2017

Support statement: This work was funded by the National Centre for the Replacement, Refinement and Reduction of Animals in Research (NC3Rs) and the Pain Relief Foundation (UK). Funding information for this article has been deposited with the Crossref Funder Registry.

Conflict of interest: Disclosures can be found alongside this article at erj.ersjournals.com

Introduction

Airway sensory nerves control cough and represent a means by which the lung clears secretions and protects itself against inhaled foreign bodies and irritants [1]. In conditions such as asthma and chronic cough this neural reflex becomes hyperresponsive, causing troublesome bouts of cough typically triggered by low level physical and chemical stimuli [2, 3]. These abnormal sensory responses often worsen during respiratory viral infections, and while the effects of virus on airway epithelial and immune cells has been extensively studied, little is known regarding the mechanisms responsible for airway neural hyperresponsiveness [4–6]. Although the symptoms associated with airway hyperresponsiveness are what disturb patients most about their condition, there are no current treatments that adequately alleviate and "reset" this state [7]. Potential therapeutic targets include the transient receptor potential (TRP) cation channels which are responsible for sensing chemical and physical stimuli and are expressed on many cell types including airway sensory nerves [8]. We have previously shown that human rhinovirus upregulates expression of TRP ankyrin 1 (TRPA1) and TRP vanilloid 1 (TRPV1) channels in a neuronally differentiated immortalised human neuroblastoma cell line [9]; however, the mechanisms involved in nerve hyperresponsiveness remain to be investigated.

A number of neuroactive molecules are released into the airway following respiratory viral infection, including nerve growth factor (NGF), which alters TRP channel function [10] and may be important in regulating airway sensory nerve responsiveness. In addition, sensory neurons are known to express Toll-like receptors (TLRs) which play a key role in host defence during microbial infection [11]. Toll-like receptor 3 (TLR 3) is of particular interest as it responds to viral double-stranded RNA (dsRNA), a by-product of replicating viruses, including rhinovirus [12], and represents a potential route through which viral infection may induce cough reflex hyperresponsiveness.

Investigating TRP channel expression and regulation in human sensory neurons is challenging because the cell bodies of peripheral neurons are housed in neuronal ganglia which are not accessible by biopsy. Although TRP channel studies have been conducted in animal models [13–15] there are recognised interspecies differences in TRP function and expression [16–18]. Furthermore, in light of European Union (EU) legislation for the protection of animals for scientific purposes there is an urgent need for development of a new generation of *in vitro* models based on human biology [19]. Thus, a human neuronal model could complement or potentially replace some animal models currently used in respiratory research and provide data that is relevant to human physiology.

Dental pulp tissue derives from migrating neural crest cells during development [20, 21] and is a source of multipotential stem/progenitor cells. The propensity for human dental pulp stem cells (hDPSCs) to differentiate towards a neuronal phenotype, previously termed peripheral neuronal equivalents (PNEs), has been reported [22–24] and is likely to be explained by their neural crest origin. Neural crest stem cells are the main contributors to the development of peripheral nerve fibres, including those of the trigeminal ganglion of the trigeminal nerve [25, 26] and jugular ganglion of the vagus nerve [27]. Jugular ganglion C-fibres terminate within the extrapulmonary airways and respond directly to tussive stimuli such as capsaicin and bradykinin, express neuropeptides and tachykinins, and are thus considered important in nociceptive airway responses such as cough. Here we describe the development of a functional human *in vitro* neuronal model differentiated from hDPSCs, suitable for studying the role of neuroinflammatory factors in TRPA1 channel-mediated neuronal hyperresponsiveness.

Methods

Full details are available in the online supplement.

Cell culture and hDPSC enrichment

Human dental pulp cells were harvested from immature permanent third molar teeth in accordance with French ethics legislation [28] and maintained in minimal essential medium-alpha (MEM-alpha) supplemented with 10% fetal bovine serum (FBS), 100 UI·mL^{-1} penicillin and 100 µg·mL^{-1} streptomycin, L-glutamine and 200 µM ascorbic acid. hDPSCs were enriched in dental pulp cell cultures by preferential adhesion to fibronectin (10 µg·mL^{-1} overnight at 4°C) coated six-well plates and incubated at 37°C for 20 min. Non-adherent cells were discarded. hDPSCs were maintained on fibronectin for 2 days in MEM-alpha.

Neural induction

hDPSCs were harvested from fibronectin-coated plates using trypsin and seeded onto plastic/glassware coated with poly-l-ornithine (0.01%) and laminin (5 µg·mL^{-1}) and incubated with neurobasal A supplemented with B27, glutaMAX, human basic fibroblast growth factor (40 ng·mL^{-1}) and epithelial growth factor (40 ng·mL^{-1}) for 7 days.

Immunofluorescence

PNEs were differentiated from hDPSCs as described above on circular coverslips (16 mm, thickness 1). Cells were washed in PBS and fixed by submerging in ice-cold acetone for 8 min then air dried. Cells were washed in PBS and blocked for nonspecific binding by incubation with 10% normal goat serum.

Cells were treated with specific primary antibody (in 10% goat serum) overnight at 4°C (table S1). Appropriate anti-species Alexa Fluor secondary antibody conjugates were diluted in PBS containing 0.1% Triton X 100 and applied to cells for 1 h at room temperature. Samples were mounted using ProLong Gold (Thermo Fisher Scientific, Paisley, UK) with DAPI and viewed using a fluorescent microscope.

qRT-PCR

Neural induction of hDPSCs towards PNEs was achieved as outlined above, except that cells were grown in 96-well plates. Total RNA was harvested using the PicoPure RNA isolation kit (Thermo Fisher Scientific) and quantified using a Take3 plate and plate reader (BioTek, Swindon, UK). RNA samples were reverse transcribed using the SuperScript VILO cDNA synthesis kit (Thermo Fisher Scientific) according to the manufacturer's instructions. qPCR reactions were set up using TaqMan universal mastermix with UNG (Thermo Fisher Scientific) according to the manufacturer's instructions using predesigned Taqman primers (Thermo Fisher Scientific; tables S2 and S3). qPCR was carried out using the Stratagene PCR instrument (Agilent, Stockport, UK) and analysed using Mx3005P software (Agilent).

Whole cell patch clamp

PNEs were differentiated as described on coverslips (thickness 0). Whole cell currents were recorded using borosilicate patch pipettes (2–5 MΩ resistance), an Axopatch 200B amplifier (Molecular Devices, Workingham, UK) and pClamp9 software (Molecular Devices).

To measure voltage-gated Na^+ channel activity, CsCl bath (150 mM NaCl, 6 mM CsCl, 1 mM $MgCl_2$, 1.5 mM $CaCl_2$, 5 mM glucose and 10 mM HEPES in dH_2O; pH altered to 7.4 using Tris) and pipette (120 mM CsCl, 1 mM $MgCl_2$, 4 mM Na_2ATP, 10 mM BAPTA and 10 mM HEPES in dH_2O; pH altered to 7.2 using Tris) solutions were used. 1 µM tetrodotoxin (TTX) was made up in CsCl bath solution. Experiments were carried out at room temperature. The holding potential was −120 mV. Current–voltage (I–V) relationships were measured using a voltage step protocol.

TRP channel activity was recorded using a CsCl bath solution and a Cs-aspartate pipette solution (100 mM $CsOH.2H_2O$, 100 mM aspartic acid, 20 mM CsCl, 1 mM $MgCl_2$, 4 mM Na_2ATP, 0.08 mM $CaCl_2$, 10 mM BAPTA and 10 mM HEPES in dH_2O; pH altered to 7.2 using Tris). 100 µM cinnamaldehyde, 10 µM HC030031, 10 µM capsaicin and 20 µM capsazepine were made up in CsCl bath solution. Experiments were carried out at 37°C. The holding potential was 0 mV throughout. I–V relationships were recorded using a voltage ramp protocol. All data were analysed using Clampfit9 software (Molecular Devices).

Microfluorimetric calcium imaging

For microfluorimetric calcium imaging, PNEs were differentiated as described on coverslips (thickness 0). PNEs were loaded with Fura-2AM (5 µM) for 40 min at 37°C, placed into a recording chamber mounted on the stage of an inverted microscope and superfused with Hanks (140 mM NaCl, 5 mM KCl, 2 mM $CaCl_2.2H_2O$, 1 mM $MgCl_2$, 10 mM HEPES free acid and 5 mM glucose in dH_2O; pH altered to 7.4 using NaOH). All solutions were kept at a 37°C using a water bath and perfusion system. $[Ca^{2+}]i$ was measured (details in supplementary material) and TRP channel activity was observed as changes in $[Ca^{2+}]i$ following stimulation with 10 µM capsaicin and 10 µM capsazepine diluted in Hanks.

Confocal Ca^{2+} imaging

PNEs were loaded with 0.4 µM fluo-4/AM for 6 min at room temperature and imaged using an iXon887 EMCCD camera (Andor Technology, Belfast, UK) coupled to a Nipkow spinning disk confocal head (CSU22, Yokogawa, Japan). A krypton-argon laser (Melles Griot UK, Ely, UK) at 488 nm was used to excite the fluo-4, and the emitted light was detected at wavelengths >510 nm. Experiments were performed using a ×60 objective (Olympus) and images were acquired at 15 frames per second. Background fluorescence from the camera, obtained using a null frame, was subtracted from each frame to obtain "F". F0 was determined as the minimum fluorescence under control conditions. The pseudo line-scan image and corresponding intensity profile plot were obtained using Image J software (NIH, Bethesda, MD, USA). $\Delta F/F0$ refers to the measurement of the change in Ca^{2+} levels from basal to peak.

ELISA

PNEs were differentiated in 96-well plates. Supernatants were collected following treatments (as outlined below) and interleukin (IL)-8 and IL-6 levels were measured using human IL-8 and IL-6 DuoSet ELISA kits (R&D Systems, Abingdon, UK) according to the manufacturer's instructions.

Treatment of PNEs

PNEs were treated with pro-inflammatory cytokines (NGF, 100 ng·mL^{-1}; IL-1β, 5 ng·mL^{-1}; tumour necrosis factor-α (TNF-α), 10 ng·mL^{-1};) and poly I:C (2 μg·mL^{-1}) for 20 min, 6 h or 24 h (table S4). Control cells were incubated with medium alone.

Results

Enriched hDPSCs undergo neuronal differentiation to become functional PNEs

hDPSCs expressed the neural crest protein markers, P75, AP2α and HNK1 (figure S1) and displayed a fibroblastic morphology consisting of splayed multipolar elongations (figure 1a). Following 7 days neuronal differentiation, cells acquired a typical bipolar neuronal morphology with a centrally located swollen cell body and axon-like projections (figure 1b). Immunofluorescence confirmed a phenotype change from hDPSC to PNE during differentiation, manifest by loss of expression of the fibroblast marker FSP (figure 1c and d) and gain of specific mature neuronal markers PGP9.5 (figure 1e and f) and synaptophysin (figure 1g and h). PNEs also expressed the neuropeptides substance P and CGRP, consistent with a sensory neuronal phenotype (figure S2).

Using whole cell patch clamping the neuronal phenotype of PNEs was further confirmed by demonstrating functional voltage-gated Na^+ (NaV) channels. Using Cs-based bath and pipette solutions to block outward K^+ currents, a family of rapidly inactivating inward currents were consistently generated when a series of 500 ms depolarising voltage steps were applied in 5 mV increments from an initial holding potential of −120 mV (figure 1i) to a final test potential of 55 mV. Currents were completely inhibited by the Na^+ channel inhibitor, TTX (1 μM) (figure 1j). Currents, normalised against cell capacitance, were plotted to show the I−V relationship (figure 1k).

Since TRPV1 has long been associated with a neuronal phenotype, its gene and protein expression in PNEs was determined by qPCR (table S5) and immunofluorescene (figure 1l). To confirm TRPV1 functionality in PNEs, whole cell patch clamping was performed using Cs^+-based bath and pipette solutions. Using a voltage ramp protocol, significant increases in both inward and outward currents were observed following application of the TRPV1 agonist capsaicin (10 μM), which were significantly inhibited by capsazepine (20 μM) (figure 1m and n). Vehicle only controls were unresponsive (figure S3). To further confirm the suitability of PNEs for functional studies, microfluorimetric $[Ca^{2+}]$i imaging was performed for TRPV1 activity. Fura-loaded PNEs were shown to demonstrate spontaneous activity (figure S4), a characteristic of functional neurons, and upon capsaicin application an instantaneous increase in PNE $[Ca^{2+}]$i was observed (figure S5a), with $[Ca^{2+}]$i levels falling immediately afterwards. In the presence of the TRPV1 antagonist, capsazepine, PNE $[Ca^{2+}]$i did not increase above basal levels (figure S5b). The change in ratio with capsaicin in the absence and presence of capsazepine was graphed for statistical analysis (figure S5c).

PNEs express functional TRPA1

Having established the neuronal phenotype of PNEs (figure 1) their suitability for studying TRPA1 channels was investigated. TRPA1 gene expression was confirmed by qPCR (table S5) along with protein expression by immunofluorescence (figure 2a). To study the functional TRPA1 on PNEs, whole cell patch clamp experiments were performed using Cs^+-based bath and pipette solutions. Using a voltage ramp protocol, significant increases in both inward and outward currents were observed in PNEs following application of cinnamaldehyde (100 μM) which were blocked by HC030031 (10 μM) (figure 2b and c). Vehicle only controls were unresponsive (figure S3). To further confirm the suitability of PNEs for functional TRPA1 studies we examined the effect of cinnamaldehyde (100 μM) on Ca^{2+} levels in single PNEs using confocal Ca^{2+} imaging. Cinnamaldehyde induced robust rises in $[Ca^{2+}]$i that were reversibly inhibited by subsequent HC030031 application (representative figures 2d and e and summary plot in figure 2f; n=9). Cinnamaldehyde responses were demonstrated to be concentration dependent (figure 2g and h), with an EC_{50} of 54 μM. Using microfluorimetric $[Ca^{2+}]$i imaging fura-loaded PNEs showed spontaneous activity (figure S4), and upon application of cinnamaldehyde an instantaneous increase in PNE $[Ca^{2+}]$i was observed (figure S6a), followed by falling $[Ca^{2+}]$i levels immediately afterwards. In the presence of HC030031, PNE $[Ca^{2+}]$i did not increase above basal levels (figure S6b). The mean change in ratio was graphed for statistical analysis (figure S6c).

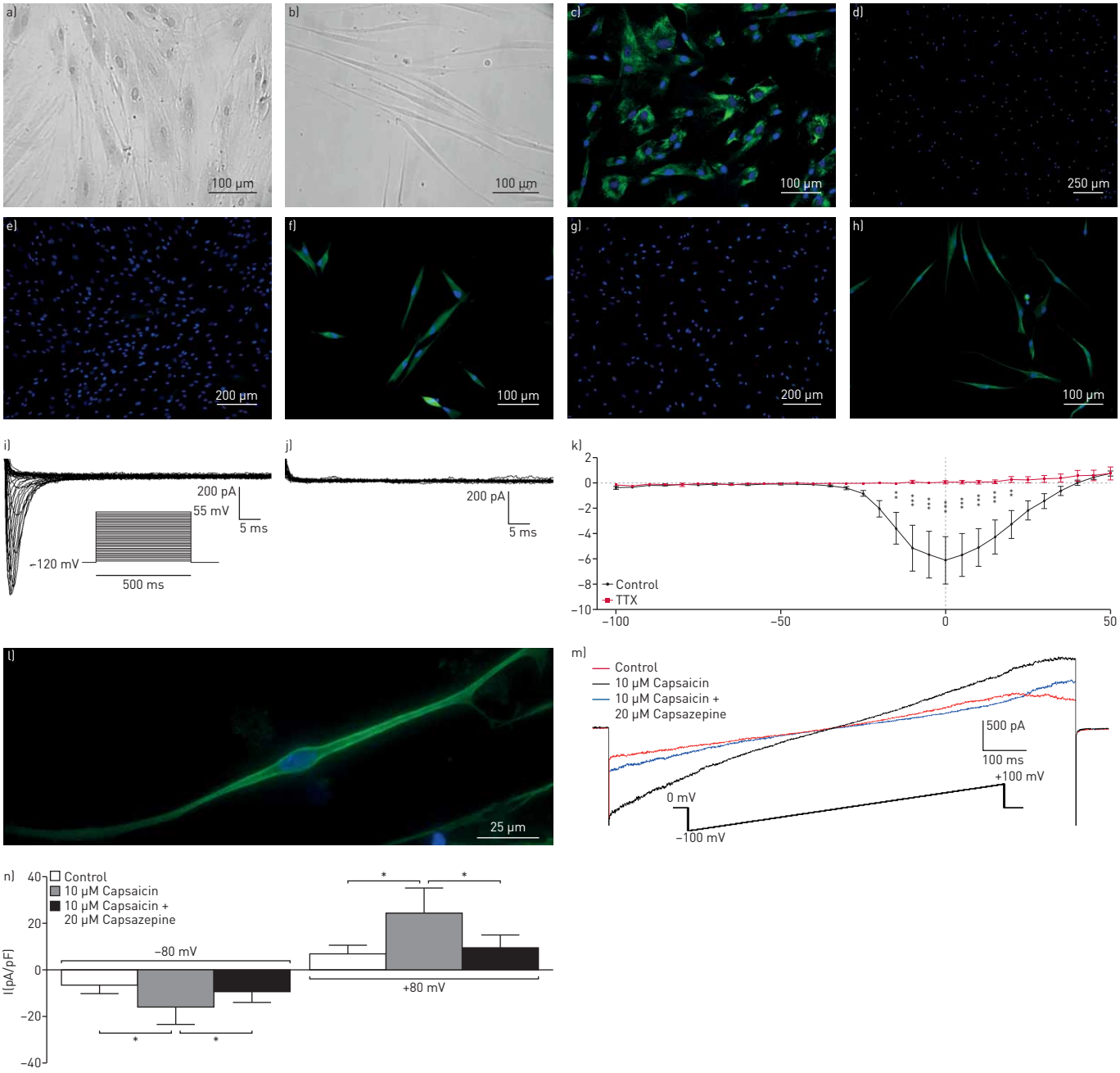

FIGURE 1 Human dental pulp stem cells (hDPSCs) undergo both morphological and phenotype changes during neuronal differentiation to become functional peripheral neuronal equivalents (PNEs). hDPSCs have a fibroblastic morphology consisting of splayed multipolar elongations (a). Following neuronal differentiation the cells lose this shape and take on a typical bipolar neuronal morphology consisting of a swollen cell body and axon-like projections (b). Undifferentiated hDPSCs express the fibroblast marker FSP (c). This FSP expression is lost during neuronal differentiation and is no longer expressed in PNEs (d). Prior to neuronal differentiation, hDPSCs do not express the specific neuronal markers PGP9.5 (e) or synaptophysin (g), which are present in PNE cultures (f and h, respectively). PNEs exhibit voltage-activated Na^+ currents following 7 days differentiation. Family of inward currents recorded from a PNE following a series of 500 ms depolarising voltage steps from an initial holding potential −120 mV to 55 mV in 5 mV increments (i). This response, in the same cells, was completely inhibited in the presence of TTX (1 µM) (j). Current–voltage relationships in the absence and presence of TTX normalised against cell capacitance (n=7; mean cell capacitance 38 pF, SEM 2.85 (measured using pClamp software)) (k). Error bars represent SEM. TRPV1 expression in PNEs was shown by immunofluorescence (l). Whole cell patch clamping recording was carried out on PNEs to investigate the functional expression of TRPV1 channels. Addition of the TRPV1 agonist capsaicin during voltage ramp protocols increased both inward and outward membrane currents. This response was inhibited in the presence of the TRPV1 antagonist capsazepine (m). Peak currents were measured at −80 mV and 80 mV for statistical analysis (n). *: p<0.05; **: p<0.01; ***: p<0.001.

NGF induces TRPA1 hyperresponsiveness on PNEs

NGF is known to induce hyperresponsiveness in sensory neurons [10, 29, 30] and is therefore a neuropathic cytokine worthy of investigating in this *in vitro* model. PNEs treated with NGF for 20 min

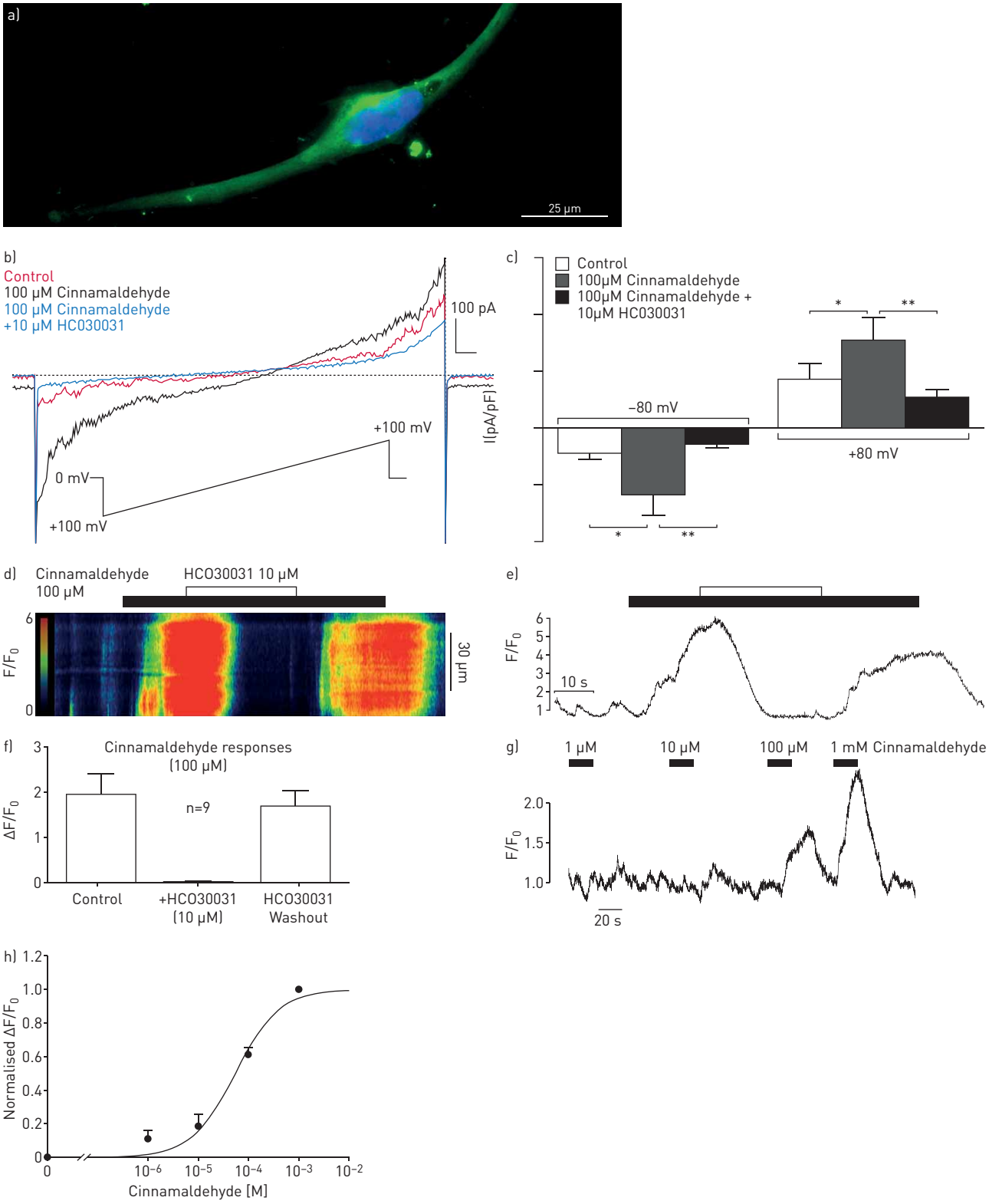

FIGURE 2 The presence of TRPA1 channel proteins in peripheral neuronal equivalents (PNEs) was confirmed using immunofluorescence (a). Whole cell patch clamping recording was carried out on PNEs to investigate the functional expression of TRPA1 channels. Addition of the TRPA1 agonist cinnamaldehyde during voltage ramp protocols increased both inward and outward membrane currents. This response was inhibited in the presence of the TRPA1 antagonist HC030031 (b). Peak currents were measured at –80 mV and 80 mV for statistical analysis (c). *: $p<0.05$; **: $p<0.01$. Application of cinnamaldehyde to isolated PNEs induced robust rises in $[Ca^{2+}]i$ that were reversibly inhibited by subsequent application of HC030031 (d and e). In nine cells the mean amplitude of cinnamaldehyde responses was significantly reduced from 1.96 $\Delta F/F_0$ under control conditions to 0.02 $\Delta F/F_0$ in the presence of HC030031; $p<0.01$, paired t-test (f). Error bars represent SEM. Cinnamaldehyde-induced elevations of $[Ca^{2+}]i$ were concentration dependent and the mean EC_{50} value for this effect was 54 µM (95% confidence intervals 38–79 µM, n=4; g and h, respectively).

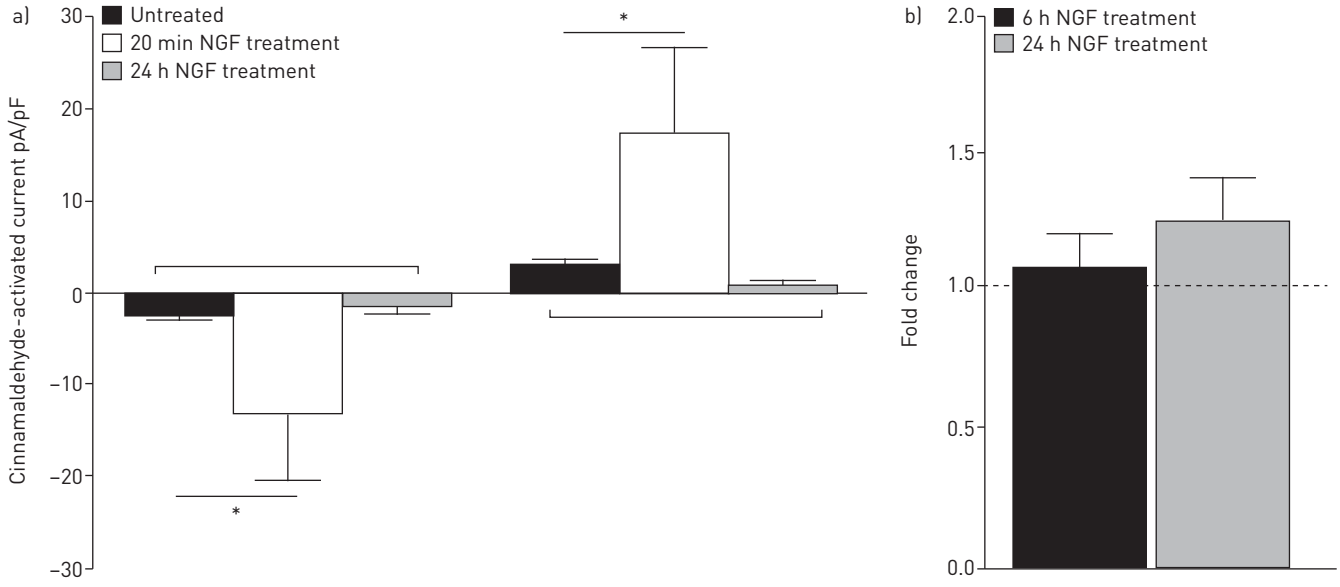

FIGURE 3 Peripheral neuronal equivalent (PNE) TRPA1 channels become hyperresponsive following 20 min incubation with the pro-inflammatory mediator nerve growth factor (NGF) (100 ng·mL^{-1}) but this effect was not apparent in PNEs incubated with NGF for 24 h; they did not show heightened responses to cinnamaldehyde (100 µM) (a). *: p<0.05. This hyperresponsiveness also appears to be independent of gene expression as no significant changes in TRPA1 gene expression in PNEs were observed following 6 h and 24 h NGF (100 ng·mL^{-1}) treatments (b).

immediately prior to patch clamp experiments generated significantly (p<0.05) larger inward and outward currents when stimulated with cinnamaldehyde (figure 3a), demonstrating that PNE TRPA1 channels hyperresponsiveness in the presence of NGF. This hyperresponsive state was not sustained, as PNEs treated for 24 h did not generate the larger currents observed previously (figure 3a).

To investigate whether TRPA1 gene expression was altered following NGF treatment we undertook qRT-PCR on PNEs incubated with NGF for 6 h and 24 h. No significant changes in TRPA1 gene expression were observed (figure 3b). To determine whether this was an NGF-specific effect, we treated PNEs with the proinflammatory cytokines TNF-α (10 ng·mL^{-1}) and IL-1β (5 ng·mL^{-1}), and observed no significant change in TRPA1 gene expression (figure S7).

We also investigated whether similar effects in response to NGF treatment were observed in PNEs stimulated with capsaicin. No significant changes in capsaicin-induced currents were seen between untreated and NGF treated cells (figure S8a). Similarly, no changes were determined in TRPV1 gene expression following NGF treatment (figure S8b).

The viral mimetic poly I:C induces IL-8 release and TRPA1 hyperresponsiveness in PNEs

Poly I:C was employed to demonstrate the usefulness of the model to investigate the effects of viral infections on sensory neurons. Cell supernatants from PNEs incubated with poly I:C were analysed for IL-8 and IL-6. Supernatants from control cells, and those incubated with poly I:C for 6 h showed no significant change in IL-8 levels, and no detectable IL-6 in controls (figure 4a and b). However, supernatants from cells incubated with poly I:C for 24 h had significantly higher levels of IL-8 (2140.8 pg·mL^{-1}) and IL-6 (246.5 pg·mL^{-1}) (figure 4a and b). Additional concentration- and time-dependent effects of poly I:C on IL-8 levels are reported in figure S9.

Poly I:C also induced TRPA1 hyperresponsiveness in PNEs. Treatment of PNEs with poly I:C for 20 min immediately prior to patch clamping generated significantly larger inward and outward currents in response to cinnamaldehyde, compared with untreated PNEs (figure 4c). PNEs incubated with poly I:C for 24 h were not readily amenable to patch clamp recording, suggesting changes had occurred in the plasma membrane. No significant changes were observed in TRPA1 gene expression following 6 h or 24 h poly I:C treatments (figure 4d).

Discussion

In this study we successfully differentiated stem cells from human dental pulp towards PNEs which have morphological, molecular and functional characteristics of sensory neurons. We observed TRPA1 channel hyperresponsiveness following stimulation with both NGF and the viral mimic poly I:C. Responses were

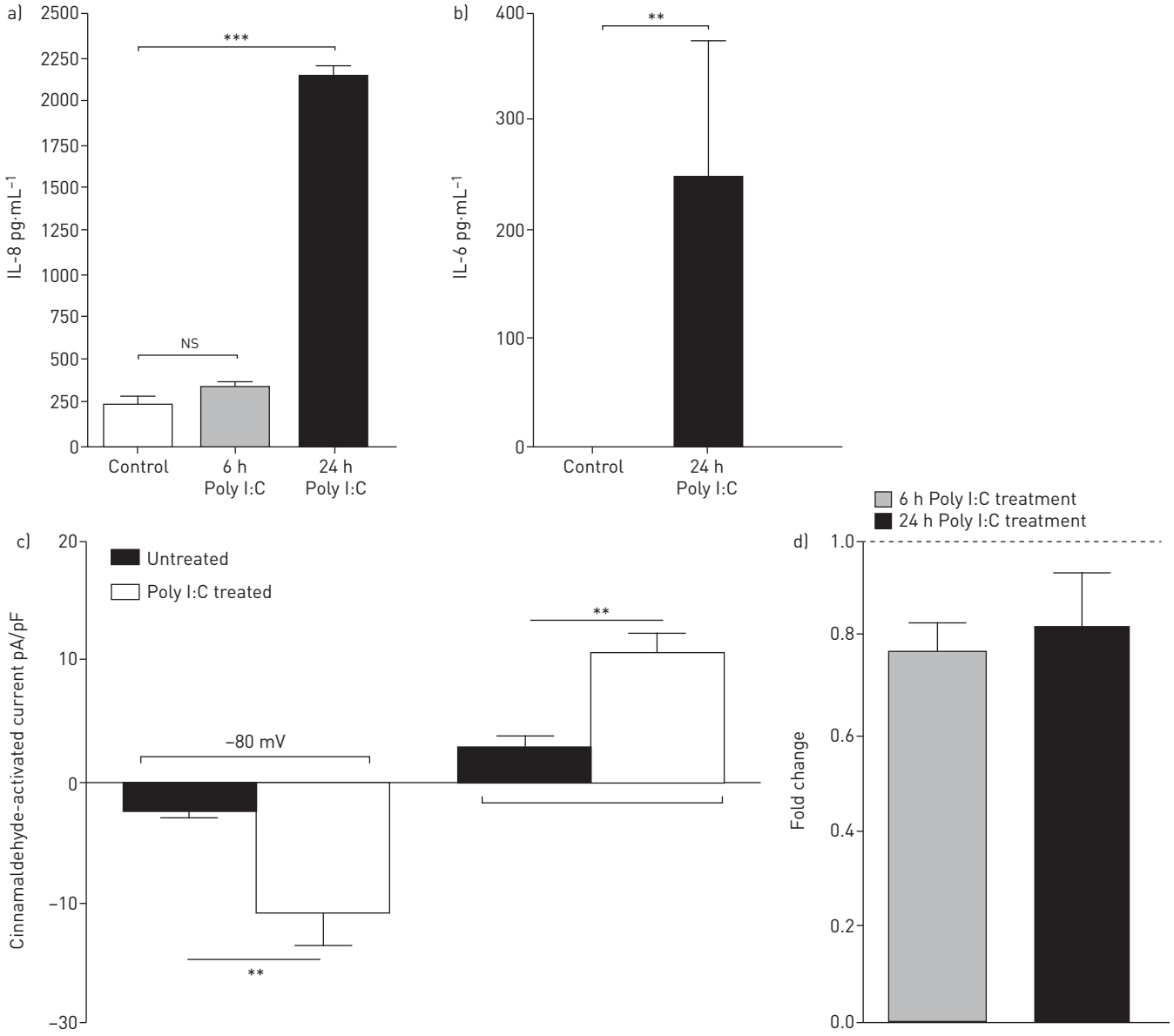

FIGURE 4 Poly I:C induces interleukin (IL)-8 and IL-6 secretion in peripheral neuronal equivalent (PNE)cultures. Supernatants taken from PNEs incubated with poly I:C (2 μg·mL^{-1}) for 24 h showed increased IL-8 and IL-6 levels than those taken from untreated PNEs or PNEs incubated with poly I:C for only 6 h (a and b, respectively). PNE TRPA1 channels become hyperresponsive following 20 min incubation with the viral mimetic poly I:C (2 μg·mL^{-1}). PNEs treated with poly I:C demonstrated heightened responses to the TRPA1 agonist cinnamaldehyde (100 μM) compared to those seen in untreated PNEs (c). This hyperresponsiveness appears to be independent of gene expression as no significant changes in TRPA1 gene expression in PNEs were observed following 6 h and 24 h poly I:C treatments (d). Bars represent SEM. *: p<0.05; **: p<0.01; ***: p<0.001.

rapid in onset, and independent of TRPA1 gene expression. Taken together, our data suggest that PNEs represent a novel, species-specific *in vitro* model for the investigation of TRPA1 channel function and regulation on human sensory neurons. We believe this model has potential to provide insight into the potential mechanisms involved in cough hypersensitivity.

An important refinement in our approach was the enrichment of hDPSCs from dental pulp cultures using differential fibronectin adhesion, allowing a phenotype switch from hDPSC to PNE in 7 days compared with 21 days previously reported using dental pulp cell cultures [22]. Functional neuronal activity in differentiated cells as described herein, should be considered a prerequisite for neuronal characterisation, particularly in view of the finding that voltage-dependent sodium channels are not present on hDPSCs [31].

To provide evidence for the suitability of PNEs as an *in vitro* model for the study of inflammatory TRP channel regulation we investigated the effect of the neurotrophic cytokine NGF. Levels of NGF are elevated

in the airways of asthmatics [32] and, in children with influenza infection, airway NGF levels are increased and correlate with disease severity and cough duration [33] We observed that NGF rapidly induced increased TRPA1 activation consistent with that reported previously in primary cultures of mouse sensory neurons [28]. Such rapid effects are likely to be due to activation of intracellular cell signalling pathways resulting in phosphorylation of the TRP channel with subsequent channel hyperresponsiveness [9]. Our data suggest NGF can rapidly induce TRPA1 channel hyperresponsiveness, supporting a role for transcription-independent mechanisms in regulating TRP responses [10]. Interestingly, we did not see increased responses to capsaicin in NGF-treated cells, previously reported in a guinea pig model *in vivo* [34]. This disparity could serve to highlight differences between animal and human tissues and may add clinical relevance to the PNE model. It is also notable that positive preclinical data in animal models of the TRPV1 antagonist XEN-D0501 sharply contrasts the lack of efficacy reported in a placebo-controlled trial in chronic cough [35].

Following PNE treatment with the viral mimic poly I:C, significant increases in IL-8 and IL-6 secretion and increased currents in response to cinnamaldehyde were observed compared to untreated PNEs. This is the first report to suggest a functional relationship between TRPA1 and poly I:C. It is known that the viral mimetic poly I:C mimics the pathogen associated molecular pattern (PAMP) dsRNA, and activates three pattern recognition receptors (PRRs) TLR3, retinoic acid-inducible gene 1 (RIG-I) and melanoma differentiation-associated protein 5 (MDA5)[36]. Functional interactions of TRPA1 and poly I:C could therefore be mediated *via* one or more of these receptors.

In conclusion, PNEs represent a novel species-specific *in vitro* model suitable for the study of TRP channel function and regulation on human sensory neurons which is in line with current EU and UK directives to replace, reduce and refine the use of animals in research [19]. Using this model we have demonstrated that NGF and the viral mimic poly I:C directly and rapidly induce a TRP channel hyperresponsiveness on the cell membranes of human sensory nerves representing a possible neuro-inflammatory process responsible for cough reflex hyperresponsiveness. We have been careful to distinguish our experimental findings of neuronal hyperresponsiveness from neuronal hypersensitivity. Under experimental neuro-inflammatory conditions we observed an increased neural response for a given stimulus which may have a clinical parallel in the form of "hypertussia" observed in patients with cough hypersensitivity syndrome (CHS) [37]. We have yet to determine if our PNE model can be rendered "hypersensitive" to low level stimulation. CHS is a disorder gaining increasing recognition amongst respiratory, allergy, gastroenterology, speech/voice and otolaryngology healthcare professionals [37]. There is a need to improve our understanding of the neurobiology of this condition and we believe the novel techniques we report in this manuscript and the clinical relevance of our experimental findings will be of interest to those working in this field.

Acknowledgements

We acknowledge the skilful technical assistance of Catherine Fulton.

References

1 Canning BJ, Chang AB, Bolser DC, *et al.* Anatomy and neurophysiology of cough: CHEST Guideline and Expert Panel report. *Chest* 2014; 146: 1633–1648.
2 Chung KF, McGarvey L, Mazzone SB. Chronic cough as a neuropathic disorder. *Lancet Respir Med* 2013; 1: 414–422.
3 Morice AH, Millqvist E, Belvisi MG, *et al.* Expert opinion on the cough hypersensitivity syndrome in respiratory medicine. *Eur Respir J* 2014; 44: 1132–1148.
4 McErlean P, Favoreto S Jr, Costa FF, *et al.* Human rhinovirus infection causes different DNA methylation changes in nasal epithelial cells from healthy and asthmatic subjects. *BMC Med Genomics* 2014; 7: 37.
5 Patel DA, You Y, Huang G, *et al.* Interferon response and respiratory virus control are preserved in bronchial epithelial cells in asthma. *J Allergy Clin Immunol* 2014; 134: 1402–1412.
6 Guo H, Baker SF, Martinez-Sobrido L, *et al.* Induction of CD8 T cell heterologous protection by a single dose of single-cycle infectious influenza virus. *J Virol* 2014; 88: 12006–12016.
7 McGarvey L, McKeagney P, Polley L, *et al.* Are there clinical features of a sensitized cough reflex? *Pulm Pharmacol Ther* 2009; 22: 59–64.
8 Bessac BF, Jordt SE. Breathtaking TRP channels: TRPA1 and TRPV1 in airway chemosensation and reflex control. *Physiology (Bethesda)* 2008; 23: 360–370.
9 Abdullah H, Heaney LG, Cosby SL, *et al.* Rhinovirus upregulates transient receptor potential channels in a human neuronal cell line: implications for respiratory virus-induced cough reflex sensitivity. *Thorax* 2014; 69: 46–54.
10 Ji RR, Samad TA, Jin SX, *et al.* p38 MAPK activation by NGF in primary sensory neurons after inflammation increases TRPV1 levels and maintains heat hyperalgesia. *Neuron* 2002; 36: 57–68.
11 Lafon M, Megret F, Lafage M, *et al.* The innate immune facet of brain: human neurons express TLR3 and sense viral dsRNA. *J Mol Neurosci* 2006; 29: 184–194.
12 Jacobs BL, Langland JO. When two strands are better than one: the mediators and modulators of the cellular responses to double-stranded RNA. *Virology* 1996; 219: 339–349.

13 Honore P, Chandran P, Hernandez G, *et al.* Repeated dosing of ABT-102, a potent and selective TRPV1 antagonist, enhances TRPV1-mediated analgesic activity in rodents, but attenuates antagonist-induced hyperthermia. *Pain* 2009; 142: 27–35.
14 Malek S, Sample SJ, Schwartz Z, *et al.* Effect of analgesic therapy on clinical outcome measures in a randomized controlled trial using client-owned dogs with hip osteoarthritis. *BMC Vet Res* 2012; 8: 185.
15 de la Roche J, Eberhardt MJ, Klinger AB, *et al.* The molecular basis for species-species activation of human TRPA1 protein by protons involves poorly conserved residues within transmembrane domains 5 and 6. *J Biol Chem* 2013; 288: 20280–20292.
16 Jordt SE, Julius D. Molecular basis for species-specific sensitivity to "hot" chilli peppers. *Cell* 2002; 108: 421–430.
17 Klionsky L, Tamir R, Gao B, *et al.* Species-specific pharmacology of Trichloro(sulfanyl)ethyl benzamides as transient receptor potential ankyrin 1 (TRPA1) antagonists. *Mol Pain* 2007; 3: 39.
18 Bianchi BR, Zhang XF, Reilly RM, *et al.* Species comparison and pharmacological characterization of human, monkey, rat, and mouse TRPA1 channels. *J Phatmacol Exp Ther* 2012; 341: 360–368.
19 European Commission Directive 2010/63/EU. Legislation for the protection of animals used for scientific purposes. Official Journal of the European Union 2010; 276: 33–79.
20 d'Aquino R, De Rosa A, Laino G, *et al.* Human dental pulp stem cells: from biology to clinical applications. *J Exp Zool B Mol Dev Evol* 2009; 312B: 408–415.
21 Coura GS, Garcez RC, de Aquiar CB, *et al.* Human periodontal ligament: a niche of neural crest stem cells. *J Periodont Res* 2008; 43: 531–536.
22 Arthur A, Rychkov G, Shi S, *et al.* Adult human dental pulp stem cells differentiate toward functionally active neurons under appropriate environmental cues. *Stem Cells* 2008; 26: 1787–1795.
23 Urraca N, Memon R, El-Iyachi I, *et al.* Characterization of neurons from immortalized dental pulp stem cells for the study of neurogenetic disorders. *Stem Cell Res* 2015; 15: 722–730.
24 Ullah I, Subbarao RB, Kim EJ, *et al.* In vitro comparative analysis of human dental stem cells from a single donor and its neuronal differentiation potential evaluated by electrophysiology. *Life Sci* 2016; 154: 39–51.
25 Trainor PA, Krumlauf R. Patterning the cranial neural crest: hindbrain segmentation and Hox gene plasticity. *Nat Rev Neurosci* 2000; 1: 116–124.
26 Cobourne MT, Mitsiadis T. Neural crest cells and patterning of the mammalian dentition. *J Exp Zool B Mol Dev Evol* 2006; 306: 251–260.
27 Thompson H, Blentic A, Watson S, *et al.* The formation of the superior and jugular ganglia: insights into the generation of sensory neurons by the neural crest. *Dev Dyn* 2010; 239: 439–445.
28 About I, Bottero MJ, De Denato P, *et al.* Human dentin production in vitro. *Exp Cell Res* 2000; 258: 33–41.
29 Anand U, Otto WR, Facer P, *et al.* TRPA1 receptor localisation in the human peripheral nervous system and functional studies in cultured human and rat sensory neurons. *Neurosci Lett* 2008; 438: 221–227.
30 Bonnington JK, McNaughton PA. Signalling pathways involved in the sensitisation of mouse nociceptive neurones by nerve growth factor. *J Physiol (Lond)* 2003; 551: 433–446.
31 Gervois P, Struys T, Hilkens P, *et al.* Neurogenic maturation of human dental pulp stem cells following neurosphere generation induces morphological and electrophysiological characteristics of functional neurons. *Stem Cells Dev* 2015; 24: 296–311.
32 Kim JS, Kang JY, Ha JH, *et al.* Expression of nerve growth factor and matrix metallopeptidase-9/tissue inhibitor of metalloproteinase-1 in asthmatic patients. *J Asthma* 2013; 50: 712–717.
33 Chiaretti A, Pulitano S, Conti G, *et al.* Interleukin and neurotrophin up-regulation correlates with the severity of H1N1 infection in children: a case-controlled study. *Int J Infect Dis* 2013; 17: e1186–e1193.
34 El-Hashim AZ, Jaffal SM. Nerve growth factor enhances cough and airway obstruction via TrkA receptor- and TRPV1-dependent mechanisms. *Thorax* 2009; 64: 791–797.
35 Belvisi MG, Birrell MA, Wortley MA, *et al.* XEN-D0501, a novel TRPV1 antagonist, does not reduce cough in refractory cough patients. *Am J Respir Crit Care Med* 2017; in press [https://doi.org/10.1164/rccm.201704-0769OC].
36 Wornle M, Sauter M, Kastenmuller K, *et al.* Novel role of toll-like receptor 3, RIG-I and MDA5 in poly (I:C) RNA-induced mesothelial inflammation. *Mol Cell Biochem* 2009; 322: 193–206.
37 Birring SS. The search for the hypersensitivity in chronic cough. *Eur Respir J* 2017; 49: 1700082.